Effective Equations for Photonic-Crystal Waveguides and Circuits

Sergei F. Mingaleev and Yuri S. Kivshar

Nonlinear Physics Group, Research School of Physical Sciences and Engineering Australian National University, Canberra ACT 0200, Australia

We suggest a novel conceptual approach for describing the properties of waveguides and circuits in photonic crystals, based on the effective discrete equations that include the long-range interaction effects. We demonstrate, on the example of sharp waveguide bends, that our approach is very effective and accurate for the study of bound states and transmission spectra of the photonic-crystal circuits, and disclose the importance of evanescent modes in their properties.

One of the most promising applications of photonic crystals is a possibility to create compact integrated optical devices [1], which would be analogous to integrated circuits in electronics, but operating entirely with light.

Usually, the properties of photonic crystals and photonic-crystal waveguides are studied by solving Maxwell's equations numerically, and such calculations are time consuming. Moreover, the numerical approach does not always provide a good physical insight. The purpose of this Letter is to suggest a novel approach, based on the effective discrete equations, for describing many of the properties of the photonic-crystal waveguides and circuits, including the example of the transmission spectra of sharp waveguide bends. The effective discrete equations we derive below are somewhat analogous to the Kirchhoff equations for electric circuits. However, in contrast to electronics, in photonic crystals both diffraction and interference become important, and thus the resulting equations involve the long-range interaction effects.

To introduce our approach, we consider a twodimensional (2D) photonic crystal consisting of infinitely long dielectric rods arranged in the form of a square lattice with the lattice spacing a. We study the light propagation in the plane normal to the rods, assuming that the rods have a radius $r_0 = 0.18a$ and the dielectric constant $\varepsilon_0 = 11.56$ (this corresponds to GaAs or Si at the wavelength $\sim 1.55 \ \mu m$). For the electric field $E(\vec{x},t) = e^{-i\omega t} E(\vec{x} \mid \omega)$ polarized parallel to the rods, Maxwell's equations reduce to the eigenvalue problem

$$\left[\nabla^2 + \left(\frac{\omega}{c}\right)^2 \varepsilon(\vec{x})\right] E(\vec{x} \,|\, \omega) = 0 \;, \tag{1}$$

which can be solved by the plane-wave method [2]. A perfect photonic crystal of this type possesses a large (38%) complete band gap (between $\omega = 0.303 \times 2\pi c/a$ and $\omega = 0.444 \times 2\pi c/a$), and it has been extensively employed during last few years for the study of bound states in waveguides and bends [3], transmission of light through sharp bends [4,5], branches [6] and channel drop filters [7], nonlinear localized modes in straight waveguides [8] and perfect photonic crystals [9]. Recently, this type of photonic crystal with a 90° bent waveguide was fabricated experimentally in macro-porous silicon with $a = 0.57 \ \mu m$ and a complete band gap at 1.55 μm [10].

To create a waveguide circuit, we introduce a system of defects and assume, for simplicity, that the defects are identical rods of the radius r_d (with ε_d) located at the points \vec{x}_m , where m is the index number of the defect rods. In the photonic crystal with defects the dielectric constant $\varepsilon(\vec{x})$ can be presented as a sum of the periodic and defect-induced terms, i.e. $\varepsilon(\vec{x}) = \varepsilon_p(\vec{x}) + \varepsilon_d(\vec{x})$, and, therefore, Eq. (1) can be written in an integral form

$$E(\vec{x} \mid \omega) = \left(\frac{\omega}{c}\right)^2 \int d^2 \vec{y} \ G(\vec{x}, \vec{y} \mid \omega) \,\varepsilon_d(\vec{y}) \, E(\vec{y} \mid \omega) , \quad (2)$$

where $G(\vec{x}, \vec{y} \mid \omega)$ is the Green function (see, e.g., [8]).

The integral equation (2) can be solved numerically in the case of a small number of the defect rods. However, such calculations become severely restricted by the current computer facilities as soon as we increase the number of the defect rods in order to create photoniccrystal waveguides, waveguide bends, and branches [4–7]. Therefore, our primary goal in this Letter is to develop a new approximate physical model that would allow the application of fast numerical techniques combined with a reasonable accuracy and the further possibility to study nonlinear photonic crystals and waveguides.

When the defects support monopole modes, a reasonably accurate model can be derived by assuming that the electric field inside a defect rod remains constant. In this case, we can average the electric field in the integral equation (2) over the cross-section of the rods [8,11], and derive an approximate matrix equation for the amplitudes of the electric field $E_n(\omega) \equiv E(\vec{x}_n | \omega)$ at the defect sites,

$$\sum_{m} M_{n,m}(\omega) E_m = 0 ,$$

$$M_{n,m}(\omega) = \varepsilon_d J_{n,m}(\omega) - \delta_{n,m} , \qquad (3)$$

where $\delta_{n,m}$ is the Dirac's delta function, and

$$J_{n,m}(\omega) = \left(\frac{\omega}{c}\right)^2 \int_{r_d} d^2 \vec{y} \ G(\vec{x}_n, \vec{x}_m + \vec{y} \,|\, \omega) \tag{4}$$

is a coupling constant determined through the Green function of a perfect 2D photonic crystal [8,9].

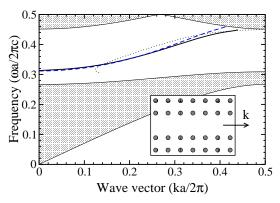


FIG. 1. Dispersion relation for the 2D photonic-crystal waveguide (shown in the inset) calculated by the super-cell method [2] (dashed), and from the approximate equations (5)-(6) for L=7 (solid) and L=1 (dotted). The gray areas are the projected band structure of a perfect 2D crystal.

To check the accuracy of the approximate model (3), first we consider a single defect located at the point \vec{x}_0 . In this case, Eq. (3) yields $J_{0,0}(\omega_d) = 1/\varepsilon_d$, and this expression defines the frequency ω_d of the defect mode. For example, applying this approach to the case when we have a defect created by a single removed rod, we obtain the frequency $\omega_d = 0.391 \times 2\pi c/a$ which differs by only 1% from the value $\omega_d = 0.387 \times 2\pi c/a$ calculated with the help of the MIT Photonic-Bands numerical code [2].

A single-mode waveguide can be created by removing a row of rods (see the inset in Fig. 1). Assuming that the waveguide is straight $(M_{n,m} \equiv M_{n-m})$ and neglecting the coupling between asunder defect rods (i.e. $M_{n-m} = 0$ for all |n - m| > L), we rewrite Eq. (3) in the transfermatrix form, $\vec{F}_{n+1} = \hat{T}\vec{F}_n$, where we introduce the vector $\vec{F}_n = \{E_n, E_{n-1}, \dots, E_{n-2L+1}\}$ and the transfer matrix $\hat{T} = \{T_{i,j}\}$ with the non-zero elements

$$T_{1,j}(\omega) = -\frac{M_{L-j}(\omega)}{M_L(\omega)} \quad \text{for} \quad j = 1, 2, ..., 2L ,$$

$$T_{j,j+1} = 1 \quad \text{for} \quad j = 1, 2, ..., 2L - 1 .$$
(5)

Solving the eigenvalue problem

$$\hat{T}(\omega)\vec{\Phi}^p = \exp\{ik_p(\omega)\}\vec{\Phi}^p, \qquad (6)$$

we can find the 2L eigenmodes of the photonic-crystal waveguide. The eigenmodes with real wavenumbers $k_p(\omega)$ correspond to the propagating waveguide modes. In the waveguide shown in Fig. 1, there exist only two such modes (we denote them as $\vec{\Phi}^1$ and $\vec{\Phi}^2$), propagating in the opposite directions ($k_1 = -k_2 > 0$). In Fig. 1 we plot the dispersion relation $k_1(\omega)$ found from Eq. (6) for the nearest-neighbor interaction (L=1) and also taking into account interaction between seven neighbors (L=7); we compare the results with those calculated directly by the super-cell method [2]. As soon as we go beyond the approximation of the nearest neighbors and take into account the coupling between several defect rods, Eqs. (3)–(6) provide very accurate results for the dispersion characteristics of the photonic-crystal waveguides. We verify that this conclusion is also valid for multi-mode waveguides, e.g. those created by removing several rows of rods.

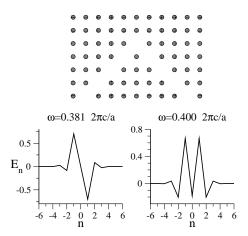


FIG. 2. Electric field E_n for two bound states supported by a 90° waveguide bend (shown in the top). Center of the bend is located at n = 0.

In addition to the propagating guided modes, in photonic-crystal waveguides there always exist *evanescent modes* with imaginary k_p . These modes, which cannot be accounted for in the framework of the nearestneighbor approximation, remain somewhat "hidden" in straight waveguides, but they become important in more elaborated structures such as waveguide bends and branches. Importantly, our model does take into account all such effects.

We consider the simplest case of a waveguide bend, where the evanescent modes manifest themselves in two different ways. First of all, they create localized bound states in the vicinity of the bend. As was shown in Ref. [3], in the cases when the waveguide bend can be considered as a finite section of a waveguide of different type, the bound states correspond closely to cavity modes excited in this finite section. However, such a simplified one-dimensional model does not describe correctly more complicated cases, even the bent waveguide depicted in Fig. 2 [3]. The situation becomes even more complicated for the waveguide branches [6]. In contrast, solving Eq. (3) we can find the frequencies and profiles of the bound states excited in an arbitrary complex set of defects. As an example, in Fig. 2 we plot the profiles of two bound states (cf. Fig. 9 in Ref. [3]). The frequencies of the modes are found from Eq. (3) with the accuracy of 1.5%.

Additionally, the evanescent modes determine the nontrivial transmission properties of the waveguide bends which can also be calculated with the help of our discrete equations. To demonstrate this, we consider a bent waveguide consisting of two coupled semi-infinite straight waveguides with a finite section (an arbitrary complex set of defects) between them. The finite section includes a bend with a safety margin of the straight waveguide at both ends. We assume that the defect rods inside this segment are characterized by the index that runs from ato b, and the amplitudes E_m (m = a, ..., b) of the electric field near the sites of the removed rods are all unknown. We number the guided modes (6) in the following way: p = 1 corresponds to the mode propagating in the direction of the waveguide bend (for both ends of the waveguide), p = 2 corresponds to the mode, propagating in the opposite direction, p = 3, ..., L + 1 correspond to the evanescent modes which grow in the direction of the bend, and p = L + 2, ..., 2L correspond to the evanescent modes which decay in the direction of the bend. Then, we can write the incoming and outcoming waves in the semi-infinite waveguide sections as a superposition of the guided modes:

$$E_m^{in} = \Phi_{a-m}^1 + r\Phi_{a-m}^2 + \sum_{p=3}^{L+1} \lambda_p^{in} \Phi_{a-m}^p , \qquad (7)$$

for m = a - 2L, ..., a - 1, and

$$E_m^{out} = t\Phi_{m-b}^2 + \sum_{p=3}^{L+1} \lambda_p^{out} \Phi_{m-b}^p , \qquad (8)$$

for m = b + 1, ..., b + 2L, where λ_p^{in} and λ_p^{out} are unknown amplitudes of the evanescent modes growing in the direction of the bend, and t and r are unknown amplitudes of the transmitted and reflected propagating waves. We take into account that the evanescent modes growing in the direction from the bend vanish, and assume that the amplitude of the incoming plane wave $\vec{\Phi}^1$ is normalized to the unity. Now, substituting Eqs. (7)–(8) into Eq. (3), we obtain a system of linear equations with 2L + b - a + 1unknown. Solving this system, we find the transmission $|t|^2$ and reflection $|r|^2$ coefficients.

In Fig. 3 we present our results for the transmission spectra of several types of bent waveguides, as in Ref. [4], where the possibility of high transmission through sharp bends in photonic-crystal waveguides was first demonstrated. As is clearly seen, Eqs. (3)-(8) provide a very accurate method for calculating the transmission spectra of the waveguide bends.

In conclusion, we have suggested a novel conceptual approach for describing the properties of photonic-crystal waveguides and circuits, including the transmission spectra of sharp bends. The effective discrete equations we have introduced here emphasize the important role of the evanescent modes in the photonic-crystal circuits, and they can be applied to study more complicated problems such as transmission in waveguide branches, channel drop filters, nonlinear localized modes in nonlinear waveguides, and so on.

The authors are indebted to S.H. Fan for useful comments and to A. Mekis for providing the data from

Ref. [4]. The work has been partially supported by the Australian Research Council.

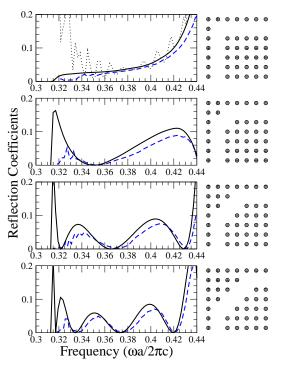


FIG. 3. Reflection coefficients calculated by the finite-difference time-domain method (dashed, from Ref. [4]) and from Eqs. (3)–(6) with L = 7 (full lines) and L = 1 (dotted, only in the top plot), for four different bend geometries.

- K. Sakoda, Optical Properties of Photonic Crystals (Springer-Verlag, Berlin, 2001); T.F. Krauss and R.M. De la Rue, Prog. Quantum Electron. 23, 51 (1999), and references therein.
- [2] S.G. Johnson and J.D. Joannopoulos, Optics Express 8, 173 (2001).
- [3] A. Mekis, S.H. Fan, and J.D. Joannopoulos, Phys. Rev. B 58, 4809 (1998).
- [4] A. Mekis, J.C. Chen, I. Kurland, S.H. Fan, P.R. Villeneuve, and J.D. Joannopoulos, Phys. Rev. Lett. 77, 3787 (1996).
- [5] S.Y. Lin, E. Chow, V. Hietala, P.R. Villeneuve, and J.D. Joannopoulos, Science 282, 274 (1998).
- [6] S. Fan, S.G. Johnson, J.D. Joannopoulos, C. Manolatou, and H.A. Haus, J. Opt. Soc. Am. B 18, 162 (2001).
- [7] S.H. Fan, P.R. Villeneuve, and J.D. Joannopoulos, Phys. Rev. Lett. 80, 960 (1998).
- [8] S.F. Mingaleev, Yu.S. Kivshar, and R.A. Sammut, Phys. Rev. E 62, 5777 (2000).
- [9] S.F. Mingaleev and Yu.S. Kivshar, Phys. Rev. Lett. 86, 5474 (2001).
- [10] T. Zijlstra, E. van der Drift, M.J.A. de Dood, E. Snoeks, and A. Polman, J. Vac. Sci. Technol. B 17, 2734 (1999).
- [11] A.R. McGurn, Phys. Rev. B 53, 7059 (1996).